Available online at www.sciencedirect.com

SciVerse ScienceDirect

Ceramics International 39 (2013) 4465–4473

CERAMICS INTERNATIONAL

www.elsevier.com/locate/ceramint

Multi-objective optimization of the parameters of TiO_2-based ceramic humidity sensors

Toshko Nenov[a], Zvezditza Nenova[b,*]

[a]Department of Automation, Information and Control Systems, Technical University of Gabrovo, 4 H.Dimitar Str., Gabrovo 5300, Bulgaria
[b]Department of Electrical Engineering, Technical University of Gabrovo, 4 H.Dimitar Str., Gabrovo 5300, Bulgaria

Received 21 October 2012; received in revised form 13 November 2012; accepted 14 November 2012
Available online 23 November 2012

Abstract

An investigation of ceramic humidity sensing elements based on titanium dioxide with dopants of PbO, Bi_2O_3 and $Na_2CO_3 \cdot 10H_2O$ has been performed. To study the complex influence of dopants and sintering temperature on the parameters and characteristics of the ceramic humidity sensors, an experimental design has been performed. A multi-objective optimization based on the method of general loss functions was carried out. The optimal composition of dopants and sintering temperature were determined to obtain ceramic sensors with optimal parameters. Experimental samples based on this optimal composition and temperature were prepared and investigated.

Keywords: C. Electrical properties; D. TiO_2; E. Sensors; Optimization

1. Introduction

Humidity measurement in gas mixtures, and in air, in particular, is a task that arises in the context of a number of scientific and technical fields. Air humidity or humidity of a technological gas is an important parameter, which influences the quality of products in many technological processes. Therefore humidity measurement plays an important role and is widely used in both research and applied activities.

This necessitates the continuous improvement of existing and development of new sensors for humidity. One of the directions of development of such sensors is the use of sensor elements based on ceramic materials. The use of ceramics for this purpose is justified by the following properties:

- ceramic microstructure is regulated fairly easily by controlling its composition and conditions of sintering;
- ceramics can be used in high temperature processes due to their thermal and environmental durability;
- ceramics are prepared under fairly simple technological processes;
- ceramics are based on inexpensive materials.

Ceramic composition and structure influence the parameters and characteristics of humidity sensors. The most important parameters of ceramic sensors are sensitivity, hysteresis of the characteristics, and response time for adsorption and desorption [1]. Another parameter which determines the possibility for connecting ceramic sensor elements to measurement circuits is their resistance at low humidity, which is usually high. All these parameters can be controlled through the sintering temperature and the use of various dopants.

One of the basic materials used for ceramic sensors is TiO_2. Under normal conditions TiO_2-based ceramics have n-type conductivity due to oxygen vacancies. The sensors of this type are prepared with the system TiO_2–V_2O_5 [2,3]. TiO_2-based sensors, doped with Nb_2O_5 have also been proposed [4]. The influence of alkaloid metals on the sensitivity of TiO_2-based ceramic sensors has been studied as well [5]. Additionally, porous ceramics based on TiO_2–$K_2Ti_6O_{13}$ have been investigated as humidity sensing elements in [6].

*Corresponding author. Tel.: +359 66 854 296; fax: +359 66 801 155.
E-mail address: z_nenova@yahoo.com (Z. Nenova).

0272-8842/$ - see front matter © 2012 Elsevier Ltd and Techna Group S.r.l. All rights reserved.
http://dx.doi.org/10.1016/j.ceramint.2012.11.040

The impact of different oxides on the sensitivity of TiO_2-based sensors has been studied in [7].

Thick film sensors based on TiO_2–SnO_2, doped with Sb_2O_5 have also been studied [8]. Investigations of thin film ceramic humidity sensors based on TiO_2–SnO_2, obtained by a sol–gel method, have been presented in [9–12]. Ceramic sensors with the same composition doped with Ta_2O_5 are investigated in [13]. Ceramic sensors based on $0.5ZrO_2$–$0.5TiO_2$ and doped with Fe_2O_3, MgO or Cr_2O_3 to 5 mol% are proposed in [14]. Sensing elements based on thick films of TiO_2–WO_3 are studied in [15]. The study in [16] covers a thick film sensor based on TiO_2–Cu_2O–Na_2O, while [17] investigates nano-crystal thin film based on Cr_2O_3–TiO_2.

TiO_2 thin films with nano-structure, doped with KCl are studied in [18]. The effect of doping with Li_2O and V_2O_5 on TiO_2-based sensors has been investigated as well [19].

In previous works [20,21], we have investigated the individual effects of Bi_2O_3, PbO and $Na_2CO_3 \cdot 10\,H_2O$, as well as the sintering temperature on the parameters of TiO_2-based humidity sensors. The three dopants are characterized by forming the respective titanates, which modify the properties of the sensing elements. However, they have ambiguous effects on the parameters of ceramic humidity sensors.

Sensing elements doped with Bi_2O_3 have the highest sensitivity and lowest response time for adsorption and desorption. Simultaneously, the hysteresis of the characteristics of these elements is higher than that of sensor elements doped with PbO, while resistivity at low humidity is higher than that of sensors doped with $Na_2CO_3 \cdot 10\,H_2O$.

The hysteresis of the characteristics of sensing elements is small for elements doped with PbO, but the adsorption and desorption time is higher than that of Bi_2O_3-doped sensors, while resistivity at low humidity is substantially larger than for sensors doped with $Na_2CO_3 \cdot 10\,H_2O$ and Bi_2O_3.

Sensor elements doped with $Na_2CO_3 \cdot 10\,H_2O$ are characterized by relatively low resistivity at low humidity but with substantial hysteresis, lower sensitivity and high response time for adsorption and desorption compared to the other two dopants.

Given the different effects of the three dopants Bi_2O_3, PbO and $Na_2CO_3 \cdot 10\,H_2O$ on the parameters and characteristics of TiO_2-based ceramic humidity sensors, the present paper presents the results of the study of their combined effects together with that of sintering temperature on the sensor parameters and characteristics. This is realized through an experimental design. The objective parameters in the investigation are the parameters of ceramic humidity sensors. A multi-objective optimization has been performed using the method of general functions of losses from the optimal values of all parameters obtained during the experimental study. The characteristics and parameters of the sensing element prepared based on the optimal composition of dopants and sintering temperature resulting from the optimization problem, have been presented as well.

2. Experimental procedure

2.1. Sample preparation

A standard ceramic technology [1] has been used to obtain the experimental samples. Homogenization is performed in a Pulverizete-5 planetary mill in a corundum pot for 4 h. Parallel to the homogenization there is milling of the oxides. After drying and granulation disc shaped samples with a 20 mm diameter and 2 mm height are pressed. The sintering temperature is different for the various samples, and the sintering time is 2 h. Prior to coating of the electrodes there is mechanical polishing of the ceramic samples, followed by cleaning of the samples in an ultrasound bath. The electrodes are obtained after burning the silver–palladium paste coated on the samples. The burning of the paste is done at 850 °C for 30 min.

2.2. Measurements

2.2.1. Surface morphology

The sample surfaces were observed by employing Scanning Electronic Microscope (SEM) Philips 525M.

2.2.2. Structural and compositional characterization was performed on the samples by XRD (X-ray diffractometry)

The measurements were performed by PHILIPS-APD15 X-ray diffractometer with CuK_α radiation.

2.2.3. Electrical characteristics and parameters

The investigated samples were placed inside a humidity generator VAPORTRON H-100BL, produced by BUCK RESEARCH INSTRUMENTS L.L.C., which provides conditioning of accurately controlled humidity with maximal deviation of up to 1.5% of relative humidity. The range of humidity used is from 30% to 93%. The resistance measurement of the samples was performed using a Precision Impedance Analyzer 6505P product of Wayne Kerr Electronics Ltd, at a 1 kHz frequency and 500 mV amplitude of the excitation signal. The influence of frequency was investigated in the range of 100 Hz to 1 MHz.

The sensitivity coefficient, K_H [7] is determined by

$$K_H = \frac{1}{RH_2 - RH_1} \ln\left(\frac{\rho_1}{\rho_2}\right), \quad (1)$$

where ρ_1 and ρ_2 is the resistivity of the sensor at a relative humidity of RH_1 and RH_2, respectively ($RH_2 > RH_1$).

The hysteresis of the sensor characteristics is determined by measuring the sensor resistivity as relative humidity rises from 30% to 93%, and then—in reverse direction. The hysteresis of the characteristics, $\rho = f(RH\%)$, is determined by

$$F = \frac{\Delta\rho_{\max}}{\rho_{FS}} \times 100\%, \quad (2)$$

where $\Delta\rho_{max}$ is the maximum difference in sensor resistivity between the sensor characteristics under humidity adsorption and desorption, and ρ_{FS} is the range of change of resistivity.

The response time for adsorption and desorption is defined as the time taken to reach a value of $(\rho_{B2}+10\%\rho_{FS})$ and $(\rho_{B1}-10\%\rho_{FS})$, respectively, where ρ_{B1} and ρ_{B2} are the resistivity values at the respective low and high base humidity levels, and ρ_{FS} is the range of change of resistivity between these levels [22]. The base relative humidity levels used are $RH_1=30\%$ and $RH_2=93\%$.

3. Experimental design for studying the properties of ceramic sensors

3.1. Determining the process control parameters of ceramic humidity sensor preparation

The following components and their boundaries of variation have been used for the investigations:

$0.70 \le TiO_2 \le 0.97$ (component $\rightarrow x_1$)

$0.01 \le PbO \le 0.10$ (component $\rightarrow x_2$)

$0.01 \le Bi_2O_3 \le 0.10$ (component $\rightarrow x_3$)

$0.01 \le Na_2CO_3.10H_2O \le 0.10$ (component $\rightarrow x_4$)

The upper bound of 0.10 for the proportion of dopants is chosen in order to have samples that are suitable for investigation. Preliminary experiments with higher fractions of PbO, Bi_2O_3 and $Na_2CO_3 \cdot 10\ H_2O$ show that some of the samples melt during sintering at temperatures from 850 °C to 1050 °C, which are used in this study. This restricts the proportion of dopants to 0.10.

The four-component composition satisfies:

$$\sum_{i=1}^{4} x_i = 1.0 \tag{3}$$

The variable factors in the experimental design are taken to be PbO, Bi_2O and $Na_2CO_3 \cdot 10\ H_2O$, while the TiO_2 component is taken as a basic component and is determined for each experiment according to the formula:

$$TiO_2 = 1—(PbO + Bi_2O_3 + Na_2CO_3 \cdot 10\ H_2O) \tag{4}$$

The sintering temperature, T°C, is chosen as a process control variable.

$850 \le T \le 1050$ °C (variable $\rightarrow x_5$).

3.2. Choice of objective parameters

The following objective parameters have been selected:

y_1—Sensitivity coefficient, K_H, $1/\%RH$;
y_2—Hysteresis, %;
y_3—Response time for adsorption, t_{ads}, s;
y_4—Response time for desorption, t_{des}, s;
y_5—Resistivity, Ωm.

The requirements towards the humidity sensor are that it has maximal sensitivity, minimal hysteresis and minimal response time for adsorption and desorption. Additionally, the requirement for a minimal resistivity at low humidity can be included for ceramic humidity sensors to facilitate easier connection to measurement circuits.

In this respect the requirements for the objective parameters are: maximal sensitivity coefficient (y_1), minimal hysteresis (y_2), minimal response time for adsorption (y_3), minimal response time for desorption (y_4), and minimal resistivity (y_5). The parameter values used have been measured at frequency of 1 kHz and temperature of 25 °C.

3.3. Experimental design

An optimal compositional design of experiments is used [23] for $n=3$ factors, which are varied at 3 levels. The main characteristic of this plan is that it guarantees a minimal variance of the predicted value of the objective parameters. The levels of the factors in the experimental design are given in Table 1. The number of experiments is

$$M = 2^n + 2n + 1 = 15. \tag{5}$$

The experimental design in coded variables is given in Table 2. This is conducted 3 times at temperatures (x_5) of 850 °C, 950 °C and 1050 °C. Table 3 shows the full experimental design in natural variables for the three

Table 1
Levels of factors in the experimental design.

Factors		Levels of the factors		
		−1 (lower)	0 (basic)	+1 (upper)
x_2	PbO	0.01	0.055	0.10
x_3	Bi_2O_3	0.01	0.055	0.10
x_4	$Na_2CO_3 \cdot 10\ H_2O$	0.01	0.055	0.10

Table 2
Experimental design.

No	Coded variables			
	x_1	$\overline{x}_2$	$\overline{x}_3$	$\overline{x}_4$
1.	−	−1	−1	−1
2.	−	−1	−1	+1
3.	−	+1	−1	−1
4.	−	+1	−1	+1
5.	−	−1	+1	−1
6.	−	−1	+1	+1
7.	−	+1	+1	−1
8.	−	+1	+1	+1
9.	−	0	0	−1
10.	−	0	0	+1
11.	−	−1	0	0
12.	−	+1	0	0
13.	−	0	−1	0
14.	−	0	+1	0
15.	−	0	0	0

Table 3
Full experimental design and experimental results.

No	x_1	x_2	x_3	x_4	x_5	y_1	y_2	y_3	y_4	y_5
	TiO_2	PbO	Bi_2O_3	$Na_2CO_3 \cdot 10\ H_2O$	T °C	K_H, $10^{-3}/\%RH$	F (%)	t_{ads}, s	t_{des}, s	ρ, 10^3 Ωm
1.	0.97	0.01	0.01	0.01	850	59.03	9.70	180	1374	9.3
2.	0.88	0.01	0.01	0.10	850	68.03	10.20	330	1448	7.9
3.	0.88	0.10	0.01	0.01	850	52.28	9.95	300	1135	7.9
4.	0.79	0.10	0.01	0.10	850	67.57	10.80	225	1047	8.3
5.	0.88	0.01	0.10	0.01	850	69.71	9.10	80	564	73.4
6.	0.79	0.01	0.10	0.10	850	64.05	9.20	300	649	7.5
7.	0.79	0.10	0.10	0.01	850	83.59	11.40	55	553	137.9
8.	0.70	0.10	0.10	0.10	850	74.08	11.71	210	668	14.5
9.	0.88	0.055	0.055	0.01	850	77.54	11.80	130	639	72.6
10.	0.79	0.055	0.055	0.10	850	67.86	10.96	355	688	8.2
11.	0.88	0.01	0.055	0.055	850	63.58	9.30	350	729	8.3
12.	0.79	0.10	0.055	0.055	850	71.45	10.30	240	619	12.2
13.	0.88	0.055	0.01	0.055	850	61.58	10.30	170	434	8.9
14.	0.79	0.055	0.10	0.055	850	79.01	10.00	130	681	24.8
15.	0.835	0.055	0.055	0.055	850	96.75	6.86	160	873	53.6
16.	0.97	0.01	0.01	0.01	950	60.33	7.64	126	904	11.7
17.	0.88	0.01	0.01	0.10	950	73.12	5.83	210	1241	15.8
18.	0.88	0.10	0.01	0.01	950	67.57	7.30	235	713	23.2
19.	0.79	0.10	0.01	0.10	950	76.27	4.74	305	1098	18.2
20.	0.88	0.01	0.10	0.01	950	73.71	13.84	265	761	301.8
21.	0.79	0.01	0.10	0.10	950	101.02	5.67	110	917	169.2
22.	0.79	0.10	0.10	0.01	950	112.94	15.96	45	1091	457.4
23.	0.70	0.10	0.10	0.10	950	111.05	4.54	65	2250	91.7
24.	0.88	0.055	0.055	0.01	950	85.55	13.05	27	1108	532.5
25.	0.79	0.055	0.055	0.10	950	82.45	7.03	206	1175	31.5
26.	0.88	0.01	0.055	0.055	950	101.36	5.11	162	1050	166.0
27.	0.79	0.10	0.055	0.055	950	131.41	3.90	95	974	1556.3
28.	0.88	0.055	0.01	0.055	950	83.08	9.23	132	713	33.7
29.	0.79	0.055	0.10	0.055	950	90.76	10.03	66	819	63.5
30.	0.835	0.055	0.055	0.055	950	131.16	4.41	12	1504	3446.0
31.	0.97	0.01	0.01	0.01	1050	52.75	22.07	536	5010	747.0
32.	0.88	0.01	0.01	0.10	1050	98.85	24.79	345	4059	730.2
33.	0.88	0.10	0.01	0.01	1050	95.42	9.81	55	520	4314.0
34.	0.79	0.10	0.01	0.10	1050	100.81	28.63	310	6794	313.8
35.	0.88	0.01	0.10	0.01	1050	59.36	13.62	85	1474	3732.7
36.	0.79	0.01	0.10	0.10	1050	102.47	10.44	135	1010	136.0
37.	0.79	0.10	0.10	0.01	1050	108.11	10.31	33	1580	3483.5
38.	0.70	0.10	0.10	0.10	1050	106.07	11.43	135	2262	161.2
39.	0.88	0.055	0.055	0.01	1050	66.64	27.92	144	762	529.2
40.	0.79	0.055	0.055	0.10	1050	97.54	17.53	270	3750	414.9
41.	0.88	0.01	0.055	0.055	1050	97.88	9.79	175	1164	104.4
42.	0.79	0.10	0.055	0.055	1050	118.37	9.58	39	958	1018.7
43.	0.88	0.055	0.01	0.055	1050	122.25	9.43	40	4467	1092.5
44.	0.79	0.055	0.10	0.055	1050	116.34	9.14	106	4759	1751.7
45.	0.835	0.055	0.055	0.055	1050	145.71	4.76	14	696	9158.2

Table 4
The best values and bounds of change for the objective parameters.

	y_1, $10^{-3}/\%RH$	y_2 (%)	y_3, s	y_4, s	y_5, 10^3 Ωm	
y_j^*	145.71	3.90	12	434	7.5	The best value for y_j of the experimental results
$y_{j\,max}$	145.71	28.63	536	6794	9158.2	The largest value for y_j of the experimental results
$y_{j\,min}$	52.28	3.90	12	434	7.5	The smallest value for y_j, of the experimental results

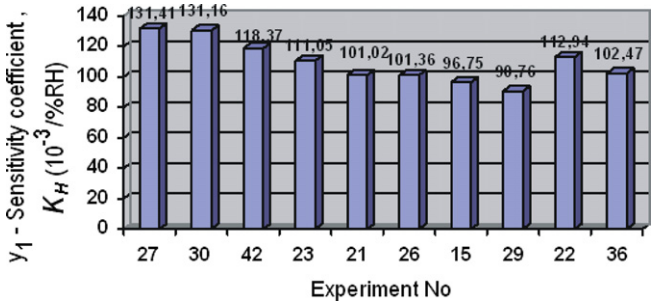

Fig. 1. Sensitivity coefficient of the ten best samples.

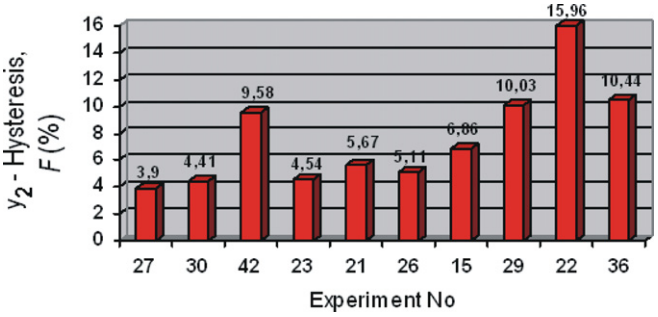

Fig. 2. Hysteresis of the ten best samples.

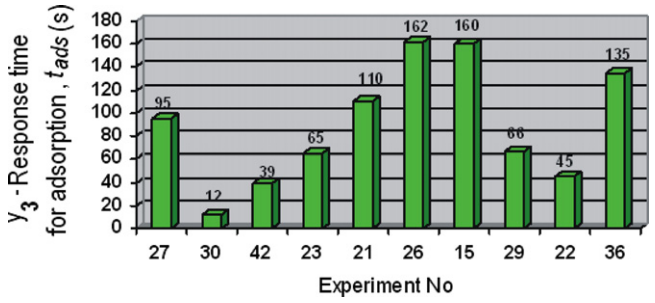

Fig. 3. Response time for adsorption of the ten best samples.

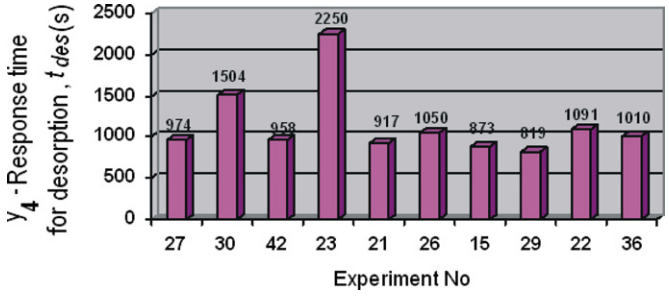

Fig. 4. Response time for desorption of the ten best samples.

temperatures and experimental results. The total number of experiments is $N=45$. The component x_1 (TiO_2) is computed according to (4).

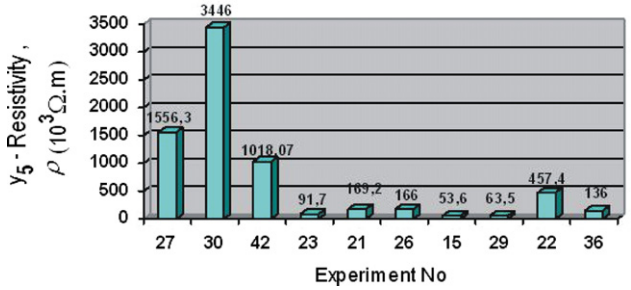

Fig. 5. Resistivity of the ten best samples.

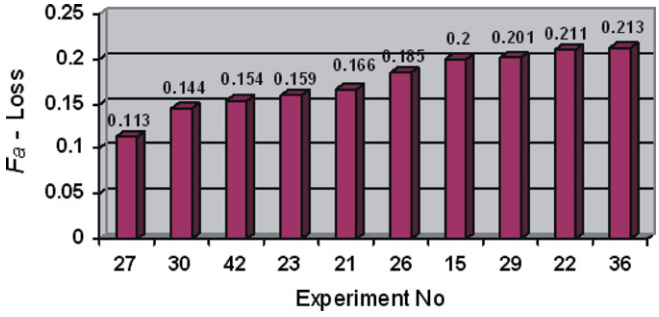

Fig. 6. Loss function of the ten best samples.

Table 5
Regression equation coefficients for the loss function F_a.

Regression coefficients
$b0=8.5476$
$b2=3.9941$
$b3=4.3692$
$b4=-2.191$
$b5=-0.018167$
$b2.2=-6.8313$
$b3.3=8.8889$
$b4.4=45.597$
$b5.5=1.012\times10^{-4}$
$b2.3=-0.1029$
$b3.4=-8.20987$
$b4.5=-3.36\times10^{-2}$
$b2.4=15.0823$
$b2.5=-4.922\times10^{-2}$
$b3.5=-6.367\times10^{-2}$
$Fu=3.7033$
$Fm_{(0.05;14;30)}=2.0374$
$R^2=0.633$

4. Multi-objective optimization of the ceramic sensor parameters

4.1. Choice of target function

Due to the opposite effects of the dopants and sintering temperature on the parameters of the sensor elements it is not possible to find an optimal composition and sintering temperature, which can give the best possible values for all

sensor parameters. That is why a compromise solution is sought simultaneously for all parameters. This is achieved by using the method of the general function of losses from the optimal values of all objective parameters obtained in the experimental investigation. This method for aggregating the vector of quality criteria is known as the optimistic approach in multi-objective optimization [24].

The normalized loss $\delta_j(x)$ of each parameter $y_j(x)$ is computed according to

$$\delta_j(x) = ABS\left(\frac{y_j^* - y_j(x)}{y_{j\,\max} - y_{j\,\min}}\right), \quad j = 1-5, \tag{6}$$

where:

y_j^* is the best result for the objective parameter $y_j(x)$ (maximum or minimum depending on the requirements for it). In the present investigation this result is chosen from the experimental results. In other cases it can be given by the requirements of a standard or norms, or as the most desirable value;

$y_j(x)$ is every experimental result from $N=45$ experiments under different composition and temperatures;

$y_{j\,\max}$ is the upper bound for normalizing the losses, which is the largest value from all experimental results for the jth objective parameter ($j=1$–5);

$y_{j\,\min}$ is the lower bound for normalizing the losses, which is the smallest value from all experimental results for the jth objective parameter ($j=1$–5).

The values for y_j^*, $y_{j\,\min}$ and $y_{j\,\max}$ are given in Table 4.

The function of losses from the best values for the objective parameters y_j ($j=1$–5) is computed according to the formula:

$$F_a(x) = \frac{1}{m}\sum_{j-1}^{m} \delta_j(x) \to \min_x \tag{7}$$

where m is the number of objective parameters ($m=5$). All parameters are given equal weights.

The losses $\delta_j(x)$ and loss function F_a are computed according to (6) and (7). Every sample (with its respective composition and sintering temperature) is given a rank depending on the value of the loss function. A rank of 1 is given to the sample with the smallest losses F_a. Samples 27,

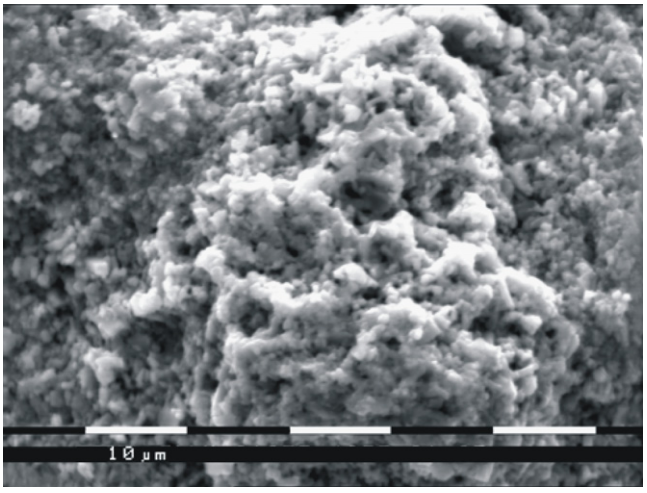

Fig. 8. SEM-image of sample 46.

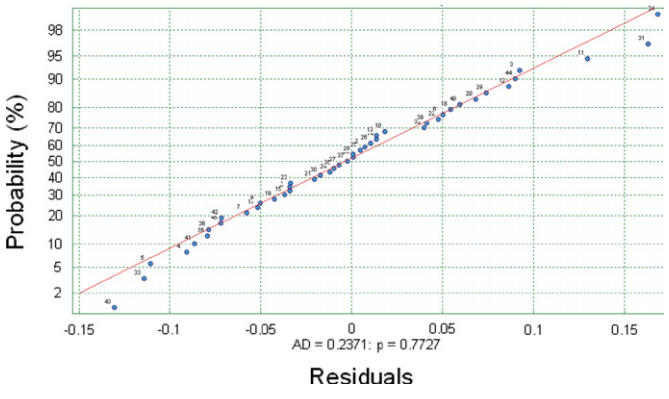

Fig. 7. Residual graph for the loss function F_a.

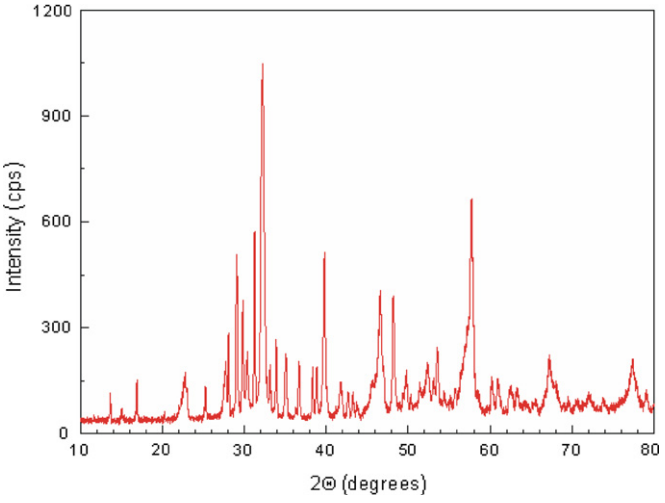

Fig. 9. X-ray diagram of sample 46.

Table 6
Optimal compromise solution.

$x_{1,\mathrm{opt}}$ TiO_2	$x_{2,\mathrm{opt}}$ PbO	$x_{3,\mathrm{opt}}$ Bi_2O_3	$x_{4,\mathrm{opt}}$ $Na_2CO_3 \cdot 10\ H_2O$	$x_{5,\mathrm{opt}}$ T, °C	$F_{a,\min}$ –
0.748	0.10	0.10	0.052	962.0	0.0833

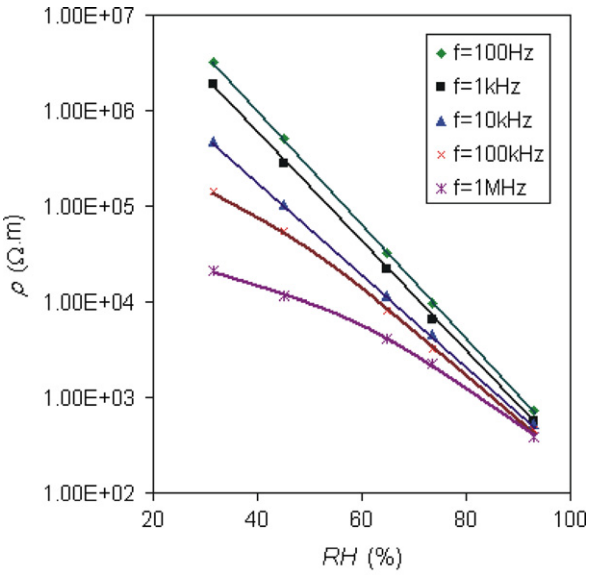

Fig. 10. Characteristics $\rho = f(RH\%)$ for sample 46.

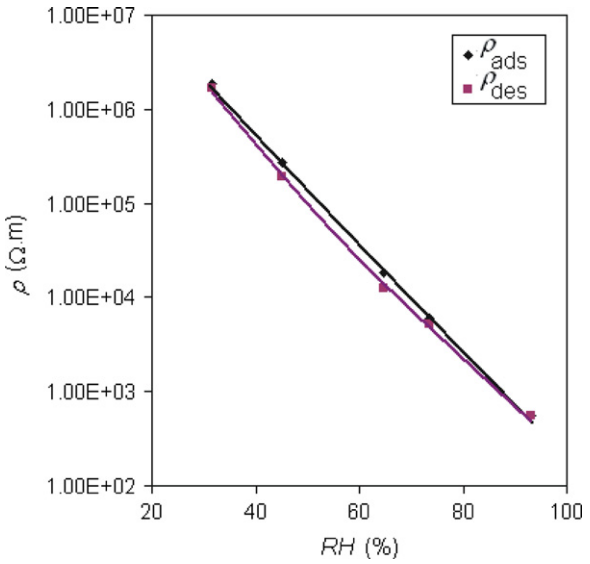

Fig. 11. Hysteresis of sample 46.

30 and 42 have the highest ranks and samples 23, 21, 26, 15, 29, 22 and 36 are in the ten best.

Figs. 1–5 give graphically the values of all parameters of the sensors from y_1 to y_5 for the ten best samples. Fig. 6 gives the loss function for the best values of all parameters for the ten best samples.

4.2. Loss function approximation

The loss function F_a is approximated by a regression equation of second order. The regression equation coefficients ($k=15$) and its statistical characteristics are given in Table 5. R^2 is the coefficient of determination. The computed value F_u of the Fisher distribution is used for a test of the significance of the multiple correlation coefficient R, and

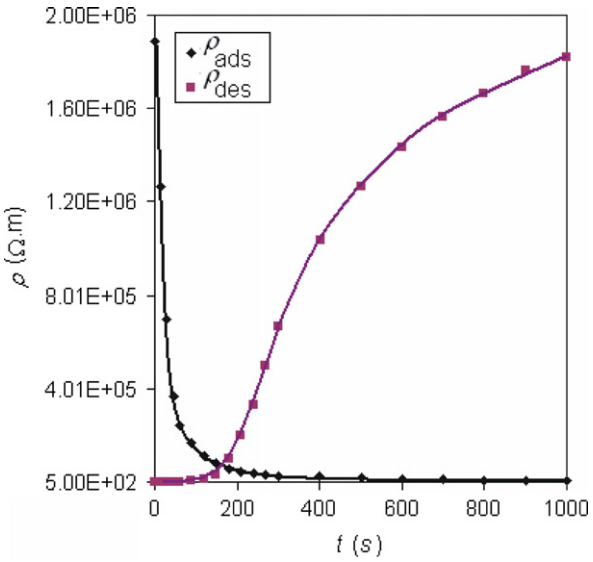

Fig. 12. Response characteristics of sample 46.

F_u is compared with the critical value $F_m(\alpha, v_1, v_2)$ of the distribution for significance level $\alpha = 0.05$ and degrees of freedom $v_1 = k-1 = 15-1 = 14$ и $v_2 = N-k = 45-15 = 30$. In that case $F_u = 3.7033 > F_{m(0.05;14;30)} = 2.0374$, which confirms the significance of the multiple correlation coefficient at that significance level. Therefore the regression equation, which describes the losses F_a has good statistical properties and can be used to determine an optimal solution for the components and sintering temperature.

The residual graph of Anderson and Darling [25] for checking the goodness-of-fit is given in Fig. 7. The actual results for F_a are fitted well by the regression equation (Table 5). The residuals are grouped very close to the reference line of the normal distribution and very few deviate substantially from it. All standardized residuals are within $\pm 2\sigma$.

4.3. Optimization results

The optimal conditions for the components and sintering temperature, which minimize the approximated loss function F_a based on the regression equation from Table 5, are determined by a genetic algorithm approach. The results are given in Table 6.

Therefore the process control regime given in Table 6 will lead to the smallest loss from the optimal value for each objective parameter.

5. Experimental results and discussion

Experimental samples using the optimal solution for dopants and sintering temperature (Table 6) have been prepared and studied. They are designated as "sample 46".

Fig. 8 presents SEM-image of sample 46, magnified 2100 times. The porous structure of the sample is observable. Such structure favors the physical adsorption of moisture.

Fig. 9 shows the XRD pattern for the investigated sample. The basic phases in the ceramics are TiO_2 (anatase) and TiO_2 (rutile) (in total around 41%). The presence of both phases of TiO_2 is related to the phase transition from anatase to rutile at over 850 °C [26]. As a result of the presence of dopants, during sintering, the respective titanates: $Bi_4Ti_3O_{12}$ (34%), $PbTiO_3$ and $PbTi_3O_7$ (19%) and smaller amounts of $Na_2Ti_6O_{13}$ (6%) have been obtained as well.

The sensor characteristics $\rho = f(RH\%)$ at different frequencies in the range of 100 Hz to 1 MHz and at the temperature of 25 °C are shown in Fig. 10. These characteristics are linear in semi-logarithmic scale within the frequency range of 100 Hz to 10 kHz. At frequencies of over 10 kHz they become non-linear in this scale and this nonlinearity grows with the increase in frequency. The sample sensitivity decreases from 139.69×10^{-3} up to 77.10×10^{-3}, 1/%RH for frequency variation from 100 Hz to 1 MHz. It should be noted that there is a very substantial change in resistivity when humidity changes and this change reaches up to about four orders at 100 Hz. When frequency increases, resistivity at low humidity decreases. For comparison with the rest of the samples, the sensitivity and resistivity of sample 46 at 1 kHz and 25 °C have been determined. They are $K_H = 132.12 \times 10^{-3}$, 1/%RH, $\rho = 565.8 \times 10^3$ Ωm, respectively.

Fig. 11 shows the characteristics of sample 46 for humidity adsorption and desorption at frequency of 1 kHz and 25 °C. On their basis the hysteresis F of the sample has been determined, which is 4.21%

Fig. 12 presents the response characteristics for adsorption and desorption. The response times for adsorption and desorption of the studied sample 46 are, respectively: $t_{ads} = 88$ s, $t_{des} = 810$ s.

The loss function value has been calculated by using the experimental values of parameters obtained for sample 46, and it is $F_a = 0.0847$. This confirms that the optimal sample has the smallest losses compared to the best ten samples, presented in Fig. 6. Compared to these samples, sample 46 has the highest sensitivity. It is almost identical to the sensitivity of the first two best samples (27 and 30), but the resistivity of sample 46 at low humidity is considerably lower than theirs. The following eight samples with the best parameters (42, 23, 21, 29, 22, 36) have lower sensitivity.

For sample 46 and the first three best samples from the experimental design, the change in resistivity, when relative humidity changes from 30% up to 93%, is over three orders of magnitude at a frequency of 1 kHz, at which the parameters are compared. For sample 29, which has the lowest sensitivity of the best ten samples ($K_H = 90.76 \times 10^{-3}$, 1/%RH), this change is also significant—in the range of over two orders. Therefore, samples based on TiO_2 doped with PbO, Bi_2O_3, and $Na_2CO_3 \cdot 10\ H_2O$ within the fixed bounds considered and sintered at a temperature of over 850 °C, have a high sensitivity to humidity.

The response time for adsorption of sample 46 has an intermediate position. Its response time for desorption is the best of the best ten samples, and its hysteresis is smaller compared to samples 42, 29 22 and 36.

6. Conclusions

An experimental design has been performed to investigate the complex influence of dopants: PbO, Bi_2O_3, $Na_2CO_3 \cdot 10\ H_2O$, and the sintering temperature on the parameters and characteristics of TiO_2 based ceramic humidity sensors. The objective parameters in the investigation are the parameters of the ceramic humidity sensors—sensitivity coefficient, hysteresis, response time for adsorption and desorption and resistivity. The experimental design has been employed at sintering temperatures of 850 °C, 950 °C and 1050 °C. A multi-objective optimization based on the objective parameters and using the method of general loss function was performed. On the basis of the optimal solution obtained, a sample was prepared and investigated. A minimum value of the loss function has been obtained for this sample, calculated on the basis of its experimentally determined parameters.

The optimal sample has the highest sensitivity, relatively low value of resistivity at low humidity, the shortest response time for desorption and intermediate values of hysteresis and response time for adsorbtion compared to the ten best samples from the experimental design. In the range of 30%RH to 93%RH the change in resistivity at frequency of 1 kHz is over three orders of magnitude.

Using the results of this investigation, different optimization problems can also be solved for subsets of the objective parameters under inequality constraints for the other parameters.

Acknowledgements

This work was supported by the National Scientific Research Fund of Bulgaria under Contract No. DO 02-148/2008.

References

[1] T. Nenov, S. Yordanov, Ceramic Sensors: Technology and Applications, Technomic Publ. Co. Inc., Lancaster–Basel, 1996.
[2] K. Katayama, T. Akiba, Rutile Humidity Sensors, Proce. Int. Meet. on Chemical Sensors, Kodansha, (1983), pp. 433–438.
[3] G. Sudo, Ceramic humidity sensor, Denshi Zairyo 19 (1980) 74–78.
[4] K. Katayama, K. Hasegawa, Y. Takanashi, T. Akira, Humidity sensitivity of Nb_2O_5-doped TiO_2 ceramics, Sensors and Actuators A 24 (1990) 55–60.
[5] K. Katayama, K. Hasegawa, T. Noda, T. Akira, H. Yanagida, Effect of alkaline oxides addition on the humidity sensitivity of Nb_2O_5—doped TiO_2, Sensors and Actuators B 2 (1990) 143–149.
[6] Y.C. Yeh, T.Y. Tseng, D.A. Chang, Electrical properties of TiO_2–$K_2Ti_{16}O_{13}$ porous ceramic humidity sensor, Journal of the American Ceramic Society 73 (1990) 1992–1998.
[7] T. Nenov, S. Yordanov, Ceramic sensor device materials, Sensors and Actuators B 8 (1992) 117–122.

[8] T. Yamamoto, Thick Film Humidity Sensor, Autumnal Conf. of Assoc. of Appl. Physics, October, (1980), 129-X-8.
[9] H.-K. Kim, S.D. Sathaye, Y.K. Hwang, S.H. Jhung, J.-S. Hwang, S.H. Kwon, S.-E. Park, J.-S. Chang, Humidity sensing properties of nanoporous TiO_2–SnO_2 ceramic sensors, Bulletin of the Korean Chemical Society 26 (2005) 1881–1884.
[10] W.-Y. Chang, Y.-C. Lin, W.-W. Ke, Y.-S. Hsieh, N.-H. Kuo, Combined TiO_2/SnO_2 material with adding Pt by sol–gel technology for humidity sensor, Materials Science Forum 505-507 (2006) 397–402.
[11] W.-P. Tai, J.-H. Oh, Fabrication and humidity sensing properties of nanostructured TiO_2–SnO_2 thin films, Sensors and Actuators B 85 (2002) 154–157.
[12] W.-Y. Chang, W.-W. Ke, Y.-S. Hsieh, N.-H. Kuo, Y.-C. Lin, Using Pt dopant and sol gel technology for sensitivity enhancement of TiO_2/SnO_2 humidity sensors, Proceedings of the 2005 IEEE Engineering in Medicine and Biology Twenty seventh Annual Conference, Shanghai, China, September 1–4, (2005), pp. 1937–1940.
[13] T. Yamamoto, H. Shimizu, Some considerations on stability of the TiO_2/SnO_2 ceramic moisture sensor, IEEE Transactions on Components, Hybrids and Manufacturing Technology 5 (1982) 238–241.
[14] S.L. Yang, J.M. Wu, ZrO_2–TiO_2 ceramic humidity sensors, Journal of Materials Science 26 (1991) 231–636.
[15] P.M. Faia, A.J. Ferreira, C.S. Furtado, Establishing and interpreting an electrical circuit representing a TiO_2–WO_3 series of humidity thick film sensors, Sensors and Actuators B 140 (2009) 128–133.
[16] D.-U. Kim, M.-S. Gong, Thick films of copper-titanate resistive humidity sensor, Sensors and Actuators B 110 (2005) 321–326.
[17] T. Jantson, T. Avarma, H. Mandar, T. Uustare, R. Jaaniso, Nanocrystalline Cr_2O_3–TiO_2 thin films by pulsed laser deposition, Sensors and Actuators B 109 (2005) 24–31.
[18] Q. Qi, Y. Feng, T. Zhang, X. Zheng, G. Lu, Influence of crystallographic structure on the humidity sensing properties of KCl-doped TiO_2 nanofibers, Sensors and Actuators B 139 (2009) 611–617.
[19] H. Aoki, Y. Azuma, T. Asaka, M. Higuchi, K. Asaga, K. Katayama, Improvement of response characteristics of TiO_2 humidity sensors by simultaneous addition of Li_2O and V_2O_5, Ceramics International 34 (2008) 819–822.
[20] T. Nenov, Z. Nenova, Humidity sensor using TiO_2–Bi_2O_3 ceramics, Nineth International Conference for Sensors, Transducers & Systems, SENSOR′99, May 18–20, 1999, Nürnberg, Proceedings, 2, (1999), pp. 641–646.
[21] T. Nenov, Humidity ceramic sensor materials on the basis of TiO_2, Third International Conference Micro Materials, MicroMat 2000, April 17–19, 2000, Berlin, Proceedings, (2000), pp. 1225–1227.
[22] G. Asch, Les Capteurs en Instrumentation Industrielle, BORDAS, Paris, 1991.
[23] I. Vuchkov, S. Stoyanov, Mathematical modelling and optimization of technological objects, Tehnika, Sofia, 1986. (in Bulgarian).
[24] S. Stoyanov, Optimization of technological processes, Tehnika, Sofia, 1993. (in Bulgarian).
[25] T.W. Anderson, D.A. Darling, A test of goodness-of-fit, Journal of the American Statistical Association 49 (1954) 765–769.
[26] D.A.H. Hanaor, C.C. Sorrell, Review of the anatase to rutile phase transformation, Journal of Materials Science 46 (2011) 855–874.